

EUV SUNSPOT PLUMES OBSERVED WITH SOHO

P. Maltby, N. Brynildsen, P. Brekke, S. V. H. Haugan, O. Kjeldseth-Moe, Ø. Wikstøl
Institute of Theoretical Astrophysics, University of Oslo, P.O. Box 1029, Blindern, 0315 Oslo, Norway
and

T. Rimmele

National Solar Observatory, Sacramento Peak, Sunspot, NM 88349, USA

ABSTRACT

Bright EUV sunspot plumes have been observed in five out of nine sunspot regions with the Coronal Diagnostic Spectrometer – CDS on SOHO. In the other four regions the brightest line emissions may appear inside the sunspot but are mainly concentrated in small regions outside the sunspot areas. These results are in contrast to those obtained during the *Solar Maximum Mission*, but are compatible with the *Skylab* mission results. The present observations show that sunspot plumes are formed in the upper part of the transition region, occur both in magnetic unipolar- and bipolar regions, and may extend from the umbra into the penumbra.

Subject headings: Sun: corona — sunspots — Sun: transition region — Sun: UV radiation

1. Introduction

Based on monochromatic EUV images obtained during the *Skylab* mission Foukal et al. (1974) introduced the notation “sunspot plumes”, defined as areas above sunspot umbrae that are “the brightest features in an active region by an order of magnitude”. This led to the idea that sunspot plumes are regions within large magnetic loops, extending to altitudes of several thousand kilometers above the photosphere, in which the temperature is one to two orders of magnitude lower than in the corona of the surrounding active region (Noyes et al. 1985). In contrast, Brueckner and Bartoe (1974) observed enhanced line emission both over plages and sunspots and Cheng, Doschek, & Feldman (1976) found that emission lines formed at temperatures below 2.4×10^5 K showed the same line emission over the sunspot as over the quiet network. Evidence against the importance of sunspot plumes came from the UVSP instrument on the *Solar Maximum Mission - SMM*. Kingston et al. (1982) found that the emission measures over the penumbrae were higher than over the umbrae. The *SMM* observations led Gurman (1993) to conclude that the umbral transition region was generally indistinguishable from the quiet transition region.

There appears to be at least two possible explanations for the discrepancy between the observations obtained with the S055 *Skylab* and the UVSP *SMM* instruments. One possibility is that sunspot plumes are formed in the upper part of the transition region and therefore are easier observed with S055 than with UVSP. Another possibility is that one type of sunspots have plumes whereas others do not. The present observations show that sunspot plumes occur both in magnetic unipolar and bipolar active regions and are most apparent in emission lines formed in the upper part of the transition region.

2. Observations and Data Reduction

Observations of nine sunspot regions (see Table 1) were obtained with the Normal Incidence Spectrometer (NIS) of the Coronal Diagnostic Spectrometer – CDS (Harrison et al. 1995), as part of a joint observing program on the Solar and Heliospheric Observatory – SOHO. A large fraction of the observing time was used to raster an area of $120'' \times 120''$, moving the narrow $2.0''$ spectrometer slit perpendicular to the slit direction in steps of $2.0''$. The exposure time was 20 s, each raster was recorded during 25 min and

Table 1: Observed active regions

NOAA	Date	θ (degrees)	Mag. Class
7973	1996 June 26	16	A
7981	1996 August 2	16	B
7986	1996 August 29	17	A
7999	1996 November 28	36	B
8011	1997 January 16	13	B
8073	1997 August 16	15	A
8076	1997 August 30	20	B
8083	1997 September 9	35	B
8085	1997 September 15	44	B

The angle θ = heliocentric angle. Magnetic field classification: A = unipolar, B = bipolar.

contains information from 60 adjacent locations for ten emission lines. Table 2 gives the line list and the corresponding ionization temperatures. For each observing sequence several rasters, up to thirteen, were obtained.

Table 2: Selected spectral lines

ID	λ (Å)	log T (K)
He I	522.2	4.3
He I	584.3	4.3
O III	599.5	5.0
O IV	554.5	5.2
O V	629.7	5.4
Ne VI	562.8	5.6
Mg VIII	315.0	5.9
Mg IX	368.0	6.0
Fe XIV	334.1	6.3
Fe XVI	360.7	6.4

The data acquisition and detector characteristics that are relevant for this study were described by Harrison et al. (1995). Briefly, the CDS data are corrected for geometrical distortions, the CCD readout bias is removed, the non-wavelength-dependent calibration parameters peculiar to the detector are applied, including the exposure time, the amplification of the microchannel plate, and a flat-field correction. The final step in calibrating is to convert the photon events into absolute units. The line parameters, peak

intensity, wavelength shift and line width are determined by a least squares fit to the observations, see Brynildsen et al. (1997). The data material consists of line profiles that are well represented by a single Gaussian shape. Small regions with complicated line profiles and regions with rapid time evolution are outside the scope of this paper.

The CDS images were coaligned with white light images using magnetograms observed with the Michelson Doppler Imager (Scherrer et al. 1995) from SOHO. To determine the location of regions with peak line intensity $I > I_p$, where I_p is a preselected value of I , we introduce the notations:

$F_U(I > I_p)$ = fraction of umbra covered with $I > I_p$,

$F_S(I > I_p)$ = fraction of sunspot covered with $I > I_p$,

$f_U(I > I_p)$ = fraction of area with $I > I_p$ located above the umbra,

$f_S(I > I_p)$ = fraction of area with $I > I_p$ located above the sunspot.

The brightest features, such as the sunspot plumes, will be located by $I > I_p = 5\bar{I}$, where \bar{I} is the average peak line intensity value within the rastered area, $120'' \times 120''$.

3. Results

In Figures 1 and 2 (Pl.00 and 00) the brightest features with peak line intensity $I > 5\bar{I}$ are encircled by yellow contours, whereas medium bright features with $I > 2.5\bar{I}$ are encircled by green contours. Below we give our reasons for identifying the brightest feature in NOAA 7986, observed on 29 August 1996 (see Fig. 1), with a sunspot plume. In contrast, Figure 2 shows that nearly all the brightest features in NOAA 7999, observed on 28 November 1996, are located outside the sunspot. The size and the location of the brightest emission features with peak line intensity $I > 5\bar{I}$ are given in Table 3 for the entire set of observations. We limit the list to the three emission lines where the sunspot plumes are most apparent.

An excellent illustration of a sunspot plume is presented in Figure 2 of Foukal et al. (1974), based on observations of McMath region 12543. To compare the brightest emission feature in NOAA 7986 (Fig. 1) with that of a sunspot plume let us first consider the variation with the line formation temperature. The line emission in the sunspot plume in McMath region 12543 exceeds that above the adjacent plage region in O iv 554 Å, O vi 1032 Å, and Ne vii 465 Å, see Fig-

ure 3 in Foukal et al. (1974). Figure 1 shows that the brightest emission above the umbra in NOAA 7986 is observed in a compatible temperature range since the brightest emission is observed in O iv 554 Å, O v 629 Å, and Ne vi 562 Å. Next consider the spatial extent of the brightest emission. According to Foukal et al. (1974) the plume's "minimum half-width is definitely smaller than the diameter of the umbra". However, their Figure 4 shows that the spatial extent changes from one emission line to another. In Ne vii 465 Å, where the plume is most apparent, the FWHM of the plume exceeds $30''$ which is considerably larger than the umbral diameter ($\approx 10''$). We find that the size of the bright features in the sunspots of NOAA 7986 and McMath region 12543 are compatible. Based on these comparisons we conclude that the sunspot in NOAA 7986 (Fig. 1) shows a sunspot plume.

A sunspot plume is located above the sunspot and is the brightest feature within the active region. It is important to note that both the extent and the location of enhanced line emission depend on the preselected intensity level I_p . We show in Figure 3 the fraction, $f_S(I > I_p)$, of the area with peak line intensity $I > I_p$ which is located above the sunspot as function of the intensity ratio, I_p/\bar{I} . For several active regions we find that as I_p/\bar{I} increases towards the brightest features an increasing fraction of the line emission in O iv 554 Å, O v 629 Å, and Ne vi 562 Å is located inside the sunspot. This means that in a search for sunspot plumes one cannot simply look for enhanced line emission, but must select the brightest regions by choosing a criterion, such as, $I > I_p = 5\bar{I}$.

If it is required that the sunspot plume must be positioned directly above the umbra, only two of the nine sunspots contain a sunspot plume. Taking into account the measured size of sunspot plumes a more reasonable requirement is that a plume is located in an area above the sunspot that includes the umbra or parts thereof and may extend into the penumbra. With this requirement the following five sunspots show plumes in O v 629 Å and Ne vi 562 Å: NOAA 7973, 7986, 8011, 8073, and 8085. In these sunspots the plumes are centered in the penumbra, the umbra (see Fig. 1), the umbra, the rim of the umbra and the penumbra, respectively. It is possible that also NOAA 8076 should be regarded as containing sunspot plumes since two of the brightest line emission regions in O v 629 Å and Ne vi 562 Å are located within the largest, leading sunspot and the third bright line emis-

sion region covers most of a following sunspot, but extends outside the sunspot. The other three active regions show bright emission both inside and outside the sunspot in Ne VI 562 Å.

Table 3: Size and location of the brightest emission regions in O IV 554 Å, O V 629 Å and Ne VI 562 Å

NOAA	ID	size (arc sec) ²	f_U	f_S $I > 5\bar{I}$	F_U	F_S
7973	O IV	7	0.00	0.00	0.00	0.00
	O V	31	0.11	0.67	0.14	0.04
	Ne VI	99	0.03	0.48	0.14	0.08
7981	O IV	384	0.03	0.42	0.03	0.10
	O V	493	0.03	0.63	0.04	0.19
	Ne VI	248	0.00	0.59	0.00	0.09
7986	O IV	105	0.26	1.00	0.80	0.21
	O V	218	0.16	0.91	1.00	0.39
	Ne VI	265	0.13	0.86	1.00	0.46
7999	O IV	156	0.00	0.00	0.00	0.00
	O V	129	0.00	0.00	0.00	0.00
	Ne VI	122	0.25	0.25	0.05	0.02
8011	O IV	0	0.00	0.00	0.00	0.00
	O V	14	0.75	0.75	0.04	0.04
	Ne VI	24	0.29	0.29	0.03	0.03
8073	O IV	3	0.00	1.00	0.00	0.01
	O V	37	0.36	0.91	0.17	0.07
	Ne VI	78	0.22	0.61	0.21	0.10
8076	O IV	54	0.06	0.12	0.03	0.01
	O V	221	0.20	0.62	0.45	0.14
	Ne VI	238	0.16	0.29	0.38	0.07
8083	O IV	377	0.06	0.26	0.08	0.08
	O V	262	0.08	0.26	0.07	0.06
	Ne VI	102	0.07	0.40	0.02	0.03
8085	O IV	102	0.10	1.00	0.07	0.09
	O V	282	0.23	0.93	0.46	0.22
	Ne VI	333	0.12	0.76	0.29	0.21

In contrast to the *SMM* observations of Gurman (1993), the present observations confirm the existence of sunspot plumes. The *SMM* observations were obtained closer to a sunspot maximum than the present observations. We cannot exclude a selection effect since the sunspots listed by Gurman (1993) are all magnetic bipolar, whereas unipolar sunspots were observed both by Foukal et al. (1974) and by us (see Table 1). However, this cannot be the entire explanation since we also observe sunspot plumes in bipolar sunspots. It appears that the CDS instrument is well suited to measure emission lines formed in the upper part of the transition region, where the sunspot plumes are most apparent. The higher sensitivity of the CDS instrument than the UVSP *SMM* instrument to line emission in this region of the solar atmosphere may be one of the reasons for the difference in results between the two instruments. The present observations suggest that sunspot plumes are formed in the upper part of the transition region, occur both

in magnetic unipolar and bipolar regions, and may extend outside the umbra and into the penumbra.

We would like to thank all the members of the large international CDS team for their extreme dedication in developing and operating this excellent instrument, the Michelson Doppler Imager team for permission to use their data for coalignment purposes and the Research Council of Norway for financial support. Data from Mees Solar Observatory, University of Hawaii, are produced with the support of NASA grant NAG 5-4941 and NASA contract NAS8-40801. SOHO is a mission of international cooperation between ESA and NASA.

REFERENCES

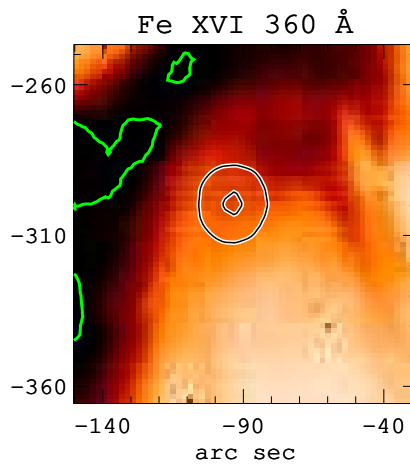
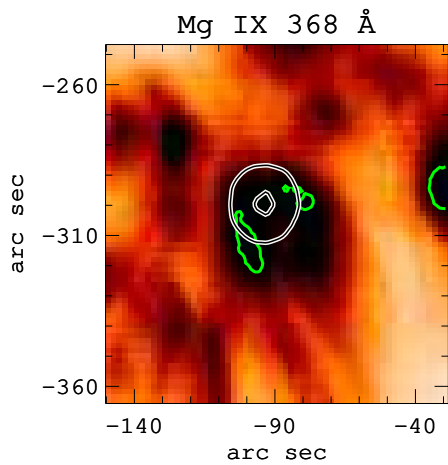
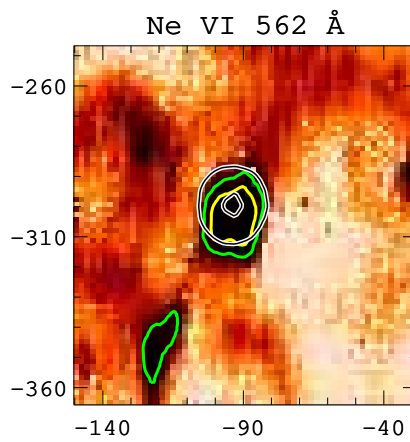
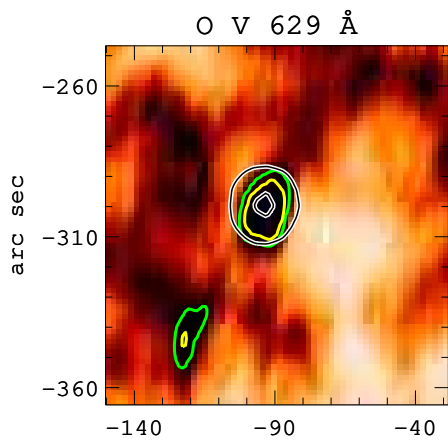
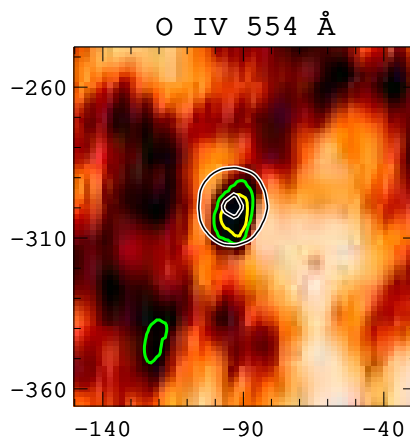
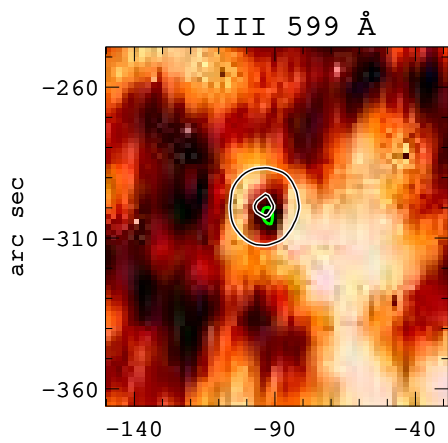
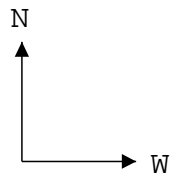
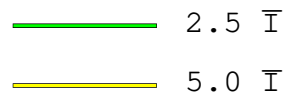
- Brueckner, G. E. and Bartoe, J.-D. F. 1974, *Solar Phys.*, 38, 133
- Brynildsen, N. et al. 1997, *Solar Phys.*, in press
- Cheng, C. C., Doschek, G., and Feldman, U. 1976, *ApJ*, 210, 836
- Foukal, P. V., Huber, M. C. E., Noyes, R. W., Reeves, E. M., Schmahl, E. J., Timothy, J. G., Vernazza, J. E., and Withbroe, G. L. 1974, *ApJ*193, L143
- Gurman, J. B. 1993, *ApJ*, 412, 865
- Harrison, R. A. et al. 1995, *Solar Phys.*, 162, 233
- Kingston, A. E., Doyle, J. G., Dufton, P.L., and Gurman, J. B. 1982, *Solar Phys.*, 81, 47
- Noyes, R. W., Raymond, J. C., Doyle, J. G., and Kingston, A. E. 1985, *ApJ*, 297, 805
- Scherrer, P. H. et al. 1995, *Solar Phys.*, 162, 129

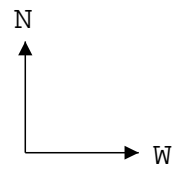
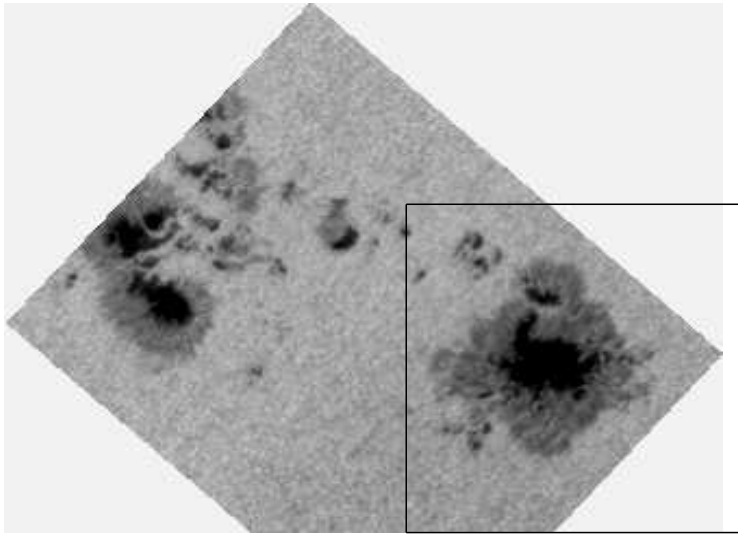
This 2-column preprint was prepared with the AAS L^AT_EX macros v4.0.

Fig. 1.— Images of peak line intensities in NOAA 7986 observed on August 29, 1996. Regions with enhanced intensity are shown as dark orange regions. Areas with peak line intensity, I , larger than 2.5 and 5 times the average intensity, \bar{I} , are encircled by green and yellow contours. The images are ordered after increasing line formation temperature, starting in the upper left hand corner. The contours of the umbra and penumbra are from white light observations at the Mees Solar Observatory, Haleakala, Hawaii. The scales in arc sec are in a reference system where the origin coincides with the centre of the solar disk.

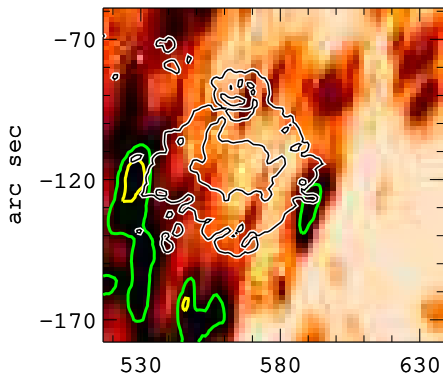
Fig. 2.— Images of peak line intensities in EUV emission lines observed on 28 November 1996. The same color code etc. as in Figure 1. White light image of NOAA 7999 observed the previous day with the Vacuum Tower Telescope at the National Solar Observatory, U.S.A. is shown (top). Only minor changes in the sunspot contour were observed from one day to the next.

Fig. 3.— The fraction, $f_S(I > I_p)$, of the area with peak line intensity $I > I_p$ that is located above the sunspot as a function of the intensity ratio I_p/\bar{I} . Note the tendency for some sunspots to show the brightest emission above sunspots in O iv 554 Å, O v 629 Å, and Ne vi 562 Å.

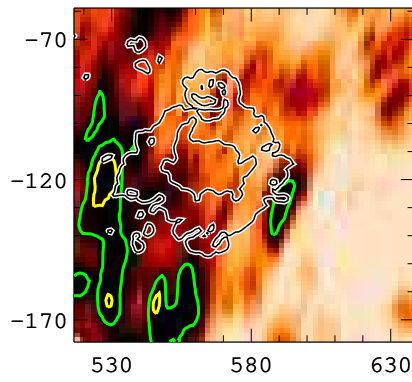




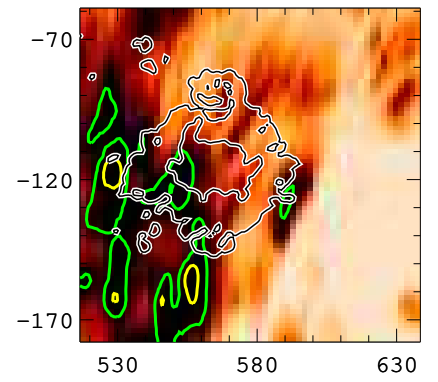
O III 599 Å



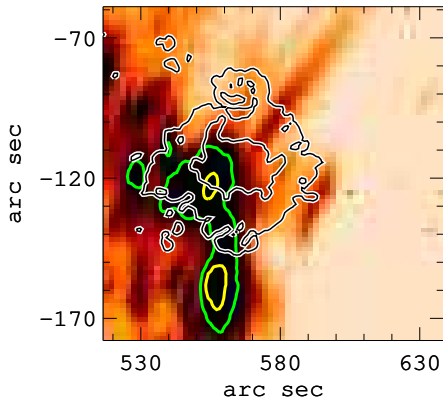
O IV 554 Å



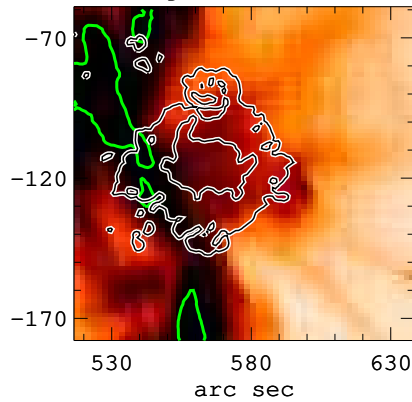
O V 629 Å



Ne VI 562 Å



Mg IX 368 Å



Fe XVI 360 Å

